THE EUROPEAN
PHYSICAL JOURNAL C

Letter

Dark matter models for the 511 keV galactic line predict keV electron recoils on Earth

Yohei Ema[1]**, Filippo Sala**[2,a] **, Ryosuke Sato**[1]

[1] DESY, Notkestraße 85, 22607 Hamburg, Germany
[2] LPTHE, CNRS, Sorbonne Université, 4 Place Jussieu, 75252 Paris, France

Abstract We propose models of Dark Matter that account for the 511 keV photon emission from the Galactic Centre, compatibly with experimental constraints and theoretical consistency, and where the relic abundance is achieved via *p*-wave annihilations or, in inelastic models, via co-annihilations. Due to the Dark Matter component that is inevitably upscattered by the Sun, these models generically predict keV electron recoils at detectors on Earth, and could naturally explain the excess recently reported by the XENON1T collaboration. The very small number of free parameters make these ideas testable by detectors like XENONnT and Panda-X, by accelerators like NA64 and LDMX, and by cosmological surveys like the Simons observatory and CMB-S4. As a byproduct of our study, we recast NA64 limits on invisibly decaying dark photons to other particles.

1 Introduction

Data that deviate from standard predictions are lifeblood of progress in physics. The past few decades have seen a plethora of such observational 'anomalies', both in cosmic rays and in underground detectors, that could have been explained by some property of particle Dark Matter (DM). None of them has been so far enough to claim the discovery of a new DM property, because of the possible alternative explanations in terms of new astrophysical sources, of underestimated systematics, etc, often flavored with a healthy dose of skepticism. An awareness has therefore emerged that the confirmation of a DM origin for some anomaly would require,

a e-mail: filo.sala@gmail.com (corresponding author)

as a necessary condition, that many anomalies are intimately linked together within a single model of DM.

It is the purpose of this letter to point out one such link. Not only we propose DM models that explain the observed 511 keV line from the Galactic Centre (GC) [1–3], but also we show they predict electron recoils with energies of the order of a keV, of the right intensity and spectrum to be observed by XENON1T [4,5] and to explain the excess seen in [5]. Our spirit in writing this paper is not to abandon the skepticism praised above, but rather to add an interesting –in our opinion– piece of information to the debates surrounding both datasets.

1.1 The 511 line and Dark Matter: preliminaries

Given that the origin of the bulge 511 keV line has not yet been clarified, and given that DM exists in our galaxy, it makes sense to entertain the possibility that the latter is responsible for the former. A DM origin for the positron injection in the bulge has indeed been investigated since [6]. The morphology of the signal excludes DM decays in favor of annihilations, see e.g. [7]. The 511 keV line emission in the galactic bulge could be accounted for by self-conjugate DM annihilations into an e^+e^- pair with

$$\langle \sigma v \rangle_{511} \simeq 5 \times 10^{-31} \left(\frac{M_{\rm DM}}{3\,{\rm MeV}}\right)^2 \frac{{\rm cm}^3}{{\rm s}}, \qquad (1)$$

where we have used the best fit provided in [7] for an NFW DM density profile, as an indicative benchmark. Different profile shapes and the use of new data for the line could change the precise value of $\langle \sigma v \rangle_{511}$, which however is not crucial for the purpose of this paper.

The need for a positron injection energy smaller than 3 MeV [8] implies that, unless one relies on cascade annihilations [9], $M_{\rm DM} \lesssim 3$ MeV. Since so small values of $M_{\rm DM}$ have been found to be in conflict with cosmological observations, a simple DM-annihilation origin of the 511 keV line

has been claimed excluded in [10]. Recently, however, the refined analysis of [11,12] found that values of M_{DM} down to ~ 1 MeV can be made consistent with CMB and BBN, by means of a small extra neutrino injection in the early universe, simultaneous with the electron one from the DM annihilations. We will rely on this new result in building DM models for the 511 keV line.

Equation (1) clarifies that s-wave DM annihilation cannot explain the 511 keV line, because so small cross sections imply overclosure of the universe. To be compatible with a thermal generation of the DM abundance, one therefore needs annihilation cross sections in the early universe much larger than today in the GC. This is realised for example in two simple pictures, where the DM relic abundance is set by:

- $\diamond$ p-wave annihilations;
- $\diamond$ coannihilations with a slightly heavier partner.

We will build explicit DM models that realise each of them in the next two paragraphs.

1.2 DM for the 511 keV line: p-wave

Using $\langle \sigma v \rangle_{\text{relic}}^{(p)}(M_{DM}{=}2\text{ MeV}) \simeq 2.2 \times 10^{-25} v_{\text{rel}}^2 \text{cm}^3/\text{s}$ [13], we find

$$M_{DM}^{(p)} \simeq 2 \text{ MeV} \frac{\langle v_{\text{rel}}^2 \rangle_{\text{bulge}}^{1/2}}{1.1 \times 10^{-3}}, \qquad (2)$$

where we have normalised $\langle v_{\text{rel}}^2 \rangle_{\text{bulge}}^{1/2}$ to the value obtained from the velocity dispersion in the bulge $\sigma \simeq 140\,\text{km/s}$ [14],[1] and where we have assumed that the dominant annihilation channel at freeze-out is e^+e^-. Note that the preferred DM mass would be the same for non-self-conjugate annihilating DM, for which both $\langle \sigma v \rangle_{511}$ and $\langle \sigma v \rangle_{\text{relic}}$ are larger by a factor of 2.

An explicit model realising this picture consists of a Majorana fermion χ as DM candidate, whose interactions with electrons are mediated by a real scalar S via the low-energy Lagrangian (we use 2 component spinor notation throughout this work)

$$\mathcal{L} = y_D \chi^2 S + g_e e_L e_R^\dagger S + \text{h.c.} \qquad (3)$$

This results in the annihilation cross section

$$\sigma v_{e^+e^-} = v_{\text{rel}}^2 \frac{(y_D g_e)^2}{8\pi} \frac{M_{DM}^2 \left(1 - m_e^2/M_{DM}^2\right)^{\frac{3}{2}}}{\left(m_S^2 - 4M_{DM}^2\right)^2 + m_S^2 \Gamma_S^2}, \qquad (4)$$

---

[1] An interesting future direction would be to refine the DM fit of the excess, by taking into account not only the radial dependence of the DM velocity dispersion (see e.g. [15,16] for old such studies), but also new data and models for the positron injection from astrophysical sources.
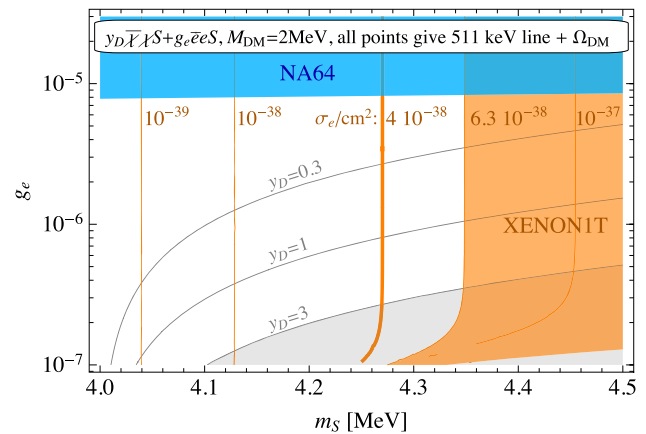
Fig. 1 Once the conditions to reproduce the DM abundance and the 511 keV line are imposed, the phenomenology of the model is entirely determined by the scalar mediator mass m_S and its coupling to electrons g_e. Shaded: non-perturbative dark coupling (gray), our recast of NA64 dark photon limit [21] (blue), indicative limit from XENON1T data [4] (orange). Lines: contours of constant σ_e (orange) and of constant dark coupling y_D (gray). The thick orange line corresponds to $\sigma_e = 4 \times 10^{-38}$ cm^2, which induces the electron recoil spectrum at XENON1T shown in Fig. 3

and in the cross section for DM-e elastic scattering

$$\sigma_e = \frac{(y_D g_e)^2}{\pi} \frac{\mu_{eDM}^2}{m_S^4}, \qquad (5)$$

where m_S is the scalar mass, Γ_S its width, and $\mu_{eDM} = m_e M_{DM}/(m_e + M_{DM})$. Once $\sigma v_{e^+e^-}$ and M_{DM} are fixed by the requirements to fit the 511 keV line Eq. (1) and to reproduce the correct relic abundance Eq. (2), then only two free parameters are left, which we choose as g_e and m_S in Fig. 1. We find that a region capable of explaining the 511 keV line exists, delimited by perturbativity, direct detection (derived later) and collider limits (see the Supplemental Material).[2]

The existence of 3 degrees of freedom with masses M_{DM} and m_S of a few MeV is not in conflict with cosmological data, provided one posits a small injection of neutrinos in the early universe in a proportion $\sim 1{:}10^4$ to the electron injection, see [11,12]. This can for example be achieved with a coupling to neutrinos, $g_\nu \nu^2 S$, of size $g_\nu \sim 10^{-2} g_e$, and where $g_e \sim 10^{-6}$ in the region allowed by the various limits, see Fig. 1. Coupling of neutrinos and electrons of these sizes can be easily obtained in electroweak-invariant completions of the Lagrangian of Eq. (3). Since they do not present any particular model-building challenge, we defer their presentation to the Supplemental Material. The results of [11,12] indicate that agreement with cosmological data fixes that ratio up to roughly one order of magnitude, so in

---

[2] Limits from CMB [17], CR electrons [18] and CR-electron-upscattered DM [19,20] do not constrain the explanation of the 511 keV line in the models presented in this paper.

this sense we do not need a very precise tuning between the electron and neutrino couplings.

Coming to future tests of this model, direct detection experiments like XENONnT and Panda-X will play a leading role in testing the available parameter space of Fig. 1. We stress that the shape of the electron recoil spectrum is fixed over the entire parameter space, only its normalisation changes according to the DD cross section shown by the orange lines. LDMX [22] will further cut in the available parameter space, as it can probe invisibly decaying dark photon with $m_V = 15$ MeV down to $\epsilon = 10^{-6}$, corresponding to g_e of the same order (see Supplemental Material). Finally, according to Ref. [12], both CMB-S4 [23] and the Simons Observatory [24] will probe $M_{\rm DM} = 2$ MeV at 95%CL or more and regardless of the ratio of the electron and neutrino couplings, thus offering useful complementary information.

1.3 DM for the 511 keV line: coannihilations

As a model that concretely realises this idea, we add to the SM a gauge group $U(1)'$, two fermions ξ and η with charges 1 and -1 respectively, and a scalar ϕ with charge 2 that spontaneously breaks the symmetry. The most general low-energy Lagrangian that preserves charge conjugation ($\eta \leftrightarrow \xi$, $\phi \leftrightarrow \phi^*$, $V_\mu \leftrightarrow -V_\mu$) reads

$$\mathcal{L} = V(|\phi|) + \frac{\epsilon}{2} V_{\mu\nu} F^{\mu\nu} + (i g_{\rm D} \chi_2^\dagger \bar\sigma_\mu \chi_1 V^\mu + \text{h.c.})$$
$$- \frac{\bar m}{2}(\chi_1^2 + \chi_2^2) - \frac{y_\phi}{2}(\phi + \phi^*)(\chi_2^2 - \chi_1^2) + \text{h.c.}, \quad (6)$$

where $\chi_1 = i(\eta - \xi)/\sqrt{2}$ and $\chi_2 = (\eta + \xi)/\sqrt{2}$ are the Majorana mass eigenstates, $F_{\mu\nu}$ is the electromagnetic field strength and we have understood all kinetic terms. The scalar mass and triple-coupling read

$$V(|\phi|) = \lambda_\phi \left(|\phi|^2 - \frac{v_\phi^2}{2}\right)^2 \Rightarrow m_\varphi^2 = 2\lambda_\phi v_\phi^2, \ \lambda_{\varphi^3} = 6\lambda_\phi v_\phi, \quad (7)$$

where $\phi = (\varphi + v_\phi)/\sqrt{2}$ and λ_{φ^3} is defined by $\mathcal{L} \supset \lambda_{\varphi^3}\varphi^3/6$. The physical vector and fermion masses read

$$m_V = 2g_{\rm D} v_\phi, \quad m_{1,2} = \bar m \pm \frac{\delta}{2}, \quad \delta = 2\sqrt{2}\, y_\phi v_\phi. \quad (8)$$

χ_1 coannihilates with χ_2 via dark photon exchange. In the limit $\delta \ll m_{1,2} = M_{\rm DM}$, one finds

$$\sigma v_{\chi_1\chi_2 \to e^+e^-} = 4\alpha_e \epsilon^2 g_{\rm D}^2 \frac{M_{\rm DM}^2 + m_e^2/2}{(m_V^2 - 4M_{\rm DM}^2)^2}\sqrt{1 - \frac{m_e^2}{M_{\rm DM}^2}}, \quad (9)$$

where α_e is the fine-structure constant. For definiteness, we then assume that χ_2 decays on cosmological scales, such that coannihilations cannot be responsible for a positron injection in the GC today. We will come back to this point in the end of the paragraph.

One can then explain the 511 keV line, if $m_\varphi < M_{\rm DM}$ and φ decays to $e\bar e$, via pair annihilations $\chi_i \chi_i \to \varphi\varphi$. The associated cross section, at first order in $y_\phi v_\phi/\lambda_{\varphi^3} \ll 1$, reads ($i = 1, 2$)

$$\sigma v_{\chi_i\chi_i \to \varphi\varphi} = v_{\rm rel}^2 \frac{y_\phi^2 \lambda_{\varphi^3}^2}{64\pi} \frac{1}{(4m_i^2 - m_\varphi^2)^2}\sqrt{1 - \frac{m_\phi^2}{m_i^2}}. \quad (10)$$

An operator $|\phi|^2(e_L e_R^\dagger + \text{h.c.})/\Lambda_{\phi e}$ with $\Lambda_{\phi e} \sim 10^{9-10} v_\phi$ guarantees that φ decays to $e\bar e$ instantaneously on astrophysical scales, while being allowed by collider, supernovae and BBN limits [25,26]. It could originate – at the price of some tuning – from a $|\phi|^2|H|^2$ term, or from the models discussed in the Supplemental Material. Since a $\chi_1\chi_1$ annihilation injects two $e\bar e$ pairs, the cross section that best fits the 511 keV line is reduced by a factor of 2 with respect to Eq. (1). Therefore we impose

$$\sigma v_{\chi_i\chi_i \to \varphi\varphi} = \frac{1}{2}\langle\sigma v\rangle_{511} \frac{v_{\rm rel}^2}{\langle v_{\rm rel}^2\rangle_{\rm bulge}}. \quad (11)$$

If $\chi_i\chi_i \to \varphi\varphi$ were the only processes responsible for the DM abundance, then we would have found another realisation of the p-wave annihilating idea, just with $M_{\rm DM} \simeq 4$ MeV.[3] It follows that, for $M_{\rm DM} \lesssim 4$ MeV, the DM relic density is set dominantly by coannihilations. We then fix ϵ by the simple requirement

$$\sigma v_{e^+e^-} + 3\frac{\sigma v_{\chi_i\chi_i \to \varphi\varphi}/v_{\rm rel}^2}{x_{\rm FO}} = \sigma v_{\rm FO}^{(s)}, \quad (12)$$

where the left-hand side sums the s- and p-wave contributions (see e.g. [27] for the origin of the relative factors) and where we use for simplicity the s-wave values at $M_{\rm DM} = 3$ MeV, $\sigma v_{\rm FO}^{(s)} \simeq 8 \times 10^{-26}$cm^3/s [13] and $x_{\rm FO} \simeq 15$ (their dependence on $M_{\rm DM}$ is very mild).

The model is then left with 4 free parameters, we visualise its parameter space in Fig. 2 for the benchmark values $m_\varphi = 2$ MeV and $m_V = 15$ MeV.[4] The allowed region is again delimited by perturbativity, direct detection and collider limits. Analogously to the previous model, these low values of $M_{\rm DM}$ can be brought in agreement with BBN and CMB data by a coupling $g_\nu V_\mu \nu^\dagger \bar\sigma^\mu \nu$, with $g_\nu \sim 10^{-2}e\epsilon$. We refer the reader to the Supplemental Material for a possible origin of g_ν. Here we just point out that it induces

---

[3] This is larger than 2 MeV of the previous section because of the factor of 2 with respect to Eq. (1) that we just explained, and because the relic cross-section is twice that of self-conjugate particles, because $\chi_1\chi_2$ cannot annihilate via $\sigma v_{\chi_i\chi_i \to \varphi\varphi}$. Note that, for $M_{\rm DM} < 6$ MeV, the positron injection energy is always smaller than the needed 3 MeV thanks to the extra step in the annihilation.

[4] The phenomenology we discuss next is not affected by their precise values, as long as $1.5 \lesssim m_\varphi/{\rm MeV} \lesssim 3$, and $10 \lesssim m_V/{\rm MeV} \lesssim 100$, where the lower limits are potentially in conflict with BBN and the upper ones close the available parameter space. Since $\bar\sigma_e$ is independent of m_V, $m_\varphi < 2$ MeV would not open any new allowed parameter space.
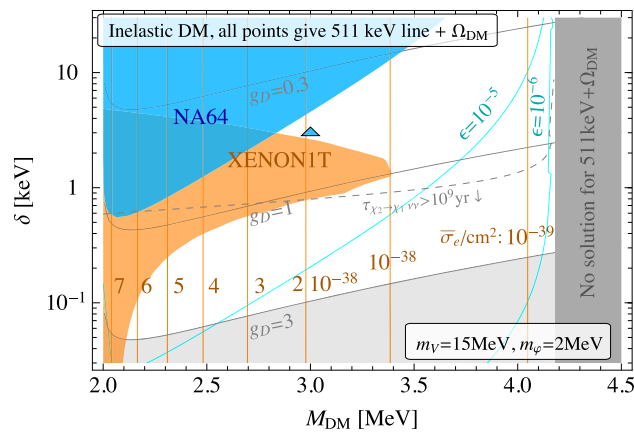
Fig. 2 The conditions to reproduce the DM abundance and the 511 keV line impose $M_{\rm DM} \lesssim 4$ MeV and leave 4 free parameters, chosen here as $M_{\rm DM}$, δ, m_φ and m_V. Shaded: non-perturbative dark coupling (gray), NA64 limit [21] (blue), indicative limit from XENON1T data [5] (orange). Lines: $\bar{\sigma}_e$ (orange), $g_{\rm D}$ (gray), ϵ (cyan). The dashed gray line roughly delimits the region where χ_2 decays into neutrinos are not enough to deplete the primordial χ_2 population, and further constraints could arise. The blue triangle corresponds to the electron recoil spectrum at XENON1T shown in Fig. 3, and it explains the excess events presented in [5]

$\Gamma_{\chi_2 \to \chi_1 \bar{\nu}\nu} \simeq g_\nu^2 g_{\rm D}^2 \delta^5/(40\pi^3 m_V^4)$, which for $m_V = 15$ MeV and $\delta \gtrsim 1$ keV implies $\tau_2 < 10^9$ years, so that all χ_2's left after freeze-out have decayed by today. Larger values of τ_2 can be avoided by adding another operator to mediate χ_2 decays (e.g. a dipole), otherwise values of $\delta \lesssim 1$ keV could potentially be in conflict with searches for the primordial population of χ_2 [28].

The allowed values of δ are restricted around a few keV, which is particularly interesting because they could explain [28] the excess events at XENON1T [5], as we explicitly derive in the next paragraph. The event rate at XENON1T is proportional to the cross section $\chi_2 e \to \chi_1 e$ in the limit $\delta \to 0$,

$$\bar{\sigma}_e = 4\alpha_e g_{\rm D}^2 \epsilon^2 \frac{\mu_{e{\rm DM}}^2}{m_V^4}, \qquad (13)$$

which we also display in Fig. 2.

Figure 2 also reports the aforementioned collider limits, and clarifies the impact that future experiments could have in testing this model. The LDMX sensitivity to dark photons will allow to almost completely probe the available parameter space. Cosmological surveys and especially DD experiments will be sensitive to a sizeable chunk of the parameter space, and thus will play an important complementary role in confirming or refuting our interpretation of the 511 keV GC line.

Finally, we left out of this study the case where there is a residual population of χ_2 today, which has also been shown to possibly explain the excess events at XENON1T [28–35].

While this goes beyond the purpose of this work, it would be interesting to investigate it in combination with the 511 keV line and we plan to come back to it in future work.

2 keV electron recoils from Sun-upscattered DM

The models we proposed to explain the 511 keV line require DM with a mass of a few MeV, interacting with electrons. Such a DM is efficiently heated inside the sun, resulting in a flux of solar-reflected DM with kinetic energy ($\sim$ keV) significantly larger than the one of halo DM, thus offering new detection avenues to direct detection experiments [36]. We now show that, via this higher-energy component, both 'p-wave' and 'coannihilations' models for the 511 keV line automatically induce electron-recoil signals that are probed by XENON1T S2-only [4] and S1+S2 [5] data.

We outline the procedure to obtain the event rate caused by the solar-reflected DM flux and refer to the Supplemental Material for more details. In the case of our interest with relatively small σ_e, the solar-reflected DM flux $\Phi_{\rm refl}$ is estimated as

$$\frac{d\Phi_{\rm refl}}{dE} \simeq \frac{n_{\rm DM}}{(1{\rm AU})^2} \int_0^{r_{\rm sun}} dr\, r^2 \frac{v_{\rm esc}(r)}{v_{\rm DM}} n_e(r) \left\langle \frac{d\sigma_e}{dE} v_e(r) \right\rangle, \qquad (14)$$

where E is the DM kinetic energy, $n_{\rm DM}$ is the DM number density, $r_{\rm sun}$ is the solar radius, $v_{\rm esc}$ is the escape velocity, $v_{\rm DM}$ is the halo DM velocity, $n_e(v_e)$ is the electron number density (velocity), and $\langle ... \rangle$ denotes the thermal average. In this formula, we have improved the analysis of [28] by including the radial dependence of the solar parameters, taken from [37]. The recoil spectrum of the electron initially in the (n, l) state of a XENON atom is given by

$$\frac{dR_{nl}}{dE_R} = \frac{N_T \sigma_e}{8\mu_{e{\rm DM}}^2 E_R} \int dq\, q\, |f_{nl}|^2 \xi(E_{\min}), \qquad (15)$$

$$\xi(E_{\min}) = \int_{E_{\min}} dE \left(\frac{M_{\rm DM}}{2E} \right) \frac{d\Phi_{\rm refl}}{dE}, \qquad (16)$$

$$E_{\min} = \frac{M_{\rm DM}}{2} \left(\frac{E_{nl} + E_R - \delta}{q} + \frac{q}{2M_{\rm DM}} \right)^2, \qquad (17)$$

where N_T is the number of target particles and E_{nl} is the electron binding energy, see e.g. [38] for a detailed derivation of the above expressions. We compute the atomic form factor f_{nl} following [32,39], and leave a refined treatment including relativistic effects [40,41] to future work.

In Fig. 3, we show the electron recoil spectra for two benchmark points $M_{\rm DM} = 2$ MeV and $\sigma_e = 4 \times 10^{-38}$ cm^2 in the p-wave case and $M_{\rm DM} = 3$ MeV, $\sigma_e = 1.9 \times 10^{-38}$ cm^2 and $\delta = 3$ keV in the coannihilation case. The induced electron recoils peak at energies below 2 keV in the p-wave
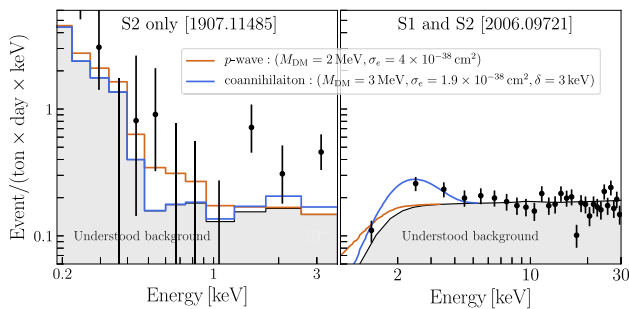
Fig. 3 Electron recoil spectra induced by solar-upscattered DM, for two benchmark values of the parameters of models that explain the 511 keV line. We overlay them with data and expected backgrounds from the XENON1T S2 [4] (left) and S1+S2 [5] (right) analyses

case, and in the coannihilation one if $\delta \lesssim$ keV. In the former case, the position of the peak is fixed by the dark matter mass Eq. (2), and it does not appear possible to explain signal excess observed at XENON1T. On the other hand, in the latter case with larger δ the events instead peak at $E_R \sim \delta$, because the downscattering $\chi_2 \to \chi_1$ releases more energy than the initial one of χ_2. In particular, the events are peaked at $E_R = 2$–3 keV in our benchmark point, which can explain the recent XENON1T anomaly. We emphasize that this result is non-trivial, because the allowed parameter region is defined by requirements and experimental limits that are completely independent of XENON1T. It is then a fortunate accident that this region is in the right ballpark for the explanation of the XENON1T anomaly.

The results of this paragraph are of course interesting beyond these anomalies, as they quantify how XENON1T tests models of light electrophilic DM. The limits shown in Figs. 1 and 2 are derived by the conservative requirement that signal plus background should not overshoot the data in [5] by more than 3σ, a more precise limit derivation is left to future work.

3 Conclusions and outlook

We have presented two models which explain the 511 keV line in the galactic bulge by annihilation of particle dark matter with a mass of order MeV. The relic abundance is set by p-wave annihilations in one model, and by coannihilations with a slightly heavier partner in the other model. We have found the novel result that these models induce electron recoils on Earth that are being tested by XENON1T, and that coannihilation models could, non-trivially, simultaneously explain the 511 keV line and the excess events recently presented by XENON1T [5]. In addition, we have demonstrated that both models are compatible with all experimental constraints, in particular with cosmological ones: to evade the conclusion of [10] that no $\mathcal{O}$(MeV) DM model could explain the 511 keV

line, we have relied on an extra annihilation channel into neutrinos and on the new results of [11,12].

Independently of the XENON1T anomaly, our proposed DM explanations of the 511 keV constitute a new physics case for experiments sensitive to keV electron recoils, like XENONnT and Panda-X [42], for accelerators like NA64 and LDMX [22], and for cosmological surveys like CMB-S4 [23] and the Simons Observatory [24]. The origin of a long-standing astrophysical mystery could be awaiting discovery in their data.

Data Availability Statement This manuscript has no associated data and no data will be deposited. [Authors' comment: This is a theoretical paper and no additional data will be deposited.]

References

1. N. Prantzos et al., The 511 keV emission from positron annihilation in the Galaxy. Rev. Mod. Phys **83**, 1001 (2011). https://doi.org/10.1103/RevModPhys.83.1001. arXiv:1009.4620
2. T. Siegert, R. Diehl, G. Khachatryan, M .G. Krause, F. Guglielmetti, J. Greiner et al., Gamma-ray spectroscopy of Positron Annihilation in the Milky Way. Astron. Astrophys **586**, A84 (2016). https://doi.org/10.1051/0004-6361/201527510. arXiv:1512.00325
3. C.A. Kierans et al., Detection of the 511 keV Galactic positron annihilation line with COSI. arXiv:1912.00110
4. XENON collaboration, Light dark matter search with ionization signals in XENON1T. Phys. Rev. Lett. **123**, 251801 (2019). https://doi.org/10.1103/PhysRevLett.123.251801. arXiv:1907.11485
5. XENON collaboration, Observation of excess electronic recoil events in XENON1T. arXiv:2006.09721
6. C. Boehm, D. Hooper, J. Silk, M. Casse, J. Paul, MeV dark matter: has it been detected? Phys. Rev. Lett **92**, 101301 (2004). https://doi.org/10.1103/PhysRevLett.92.101301. arXiv:astro-ph/0309686
7. A.C. Vincent, P. Martin, J.M. Cline, Interacting dark matter contribution to the Galactic 511 keV gamma ray emission: constraining the morphology with INTEGRAL/SPI observations. JCAP **04**, 022 (2012). https://doi.org/10.1088/1475-7516/2012/04/022. arXiv:1201.0997

8. J .F. Beacom, H. Yuksel, Stringent constraint on galactic positron production. Phys. Rev. Lett **97**, 071102 (2006). https://doi.org/10.1103/PhysRevLett.97.071102. arXiv:astro-ph/0512411

9. L.-B. Jia, Explanation of the 511 keV line: cascade annihilating dark matter with the ^{8} Be anomaly. Eur. Phys. J. C **78**, 112 (2018). https://doi.org/10.1140/epjc/s10052-018-5555-0. arXiv:1710.03906

10. R .J. Wilkinson, A .C. Vincent, C. Bœhm, C. McCabe, Ruling out the light weakly interacting massive particle explanation of the Galactic 511 keV line. Phys. Rev. D **94**, 103525 (2016). https://doi.org/10.1103/PhysRevD.94.103525. arXiv:1602.01114

11. M. Escudero, Neutrino decoupling beyond the Standard Model: CMB constraints on the Dark Matter mass with a fast and precise N_{eff} evaluation. JCAP **02**, 007 (2019). https://doi.org/10.1088/1475-7516/2019/02/007. arXiv:1812.05605

12. N. Sabti, J. Alvey, M. Escudero, M. Fairbairn, D. Blas, Refined bounds on MeV-scale thermal dark sectors from BBN and the CMB. JCAP **2001**, 004 (2020). https://doi.org/10.1088/1475-7516/2020/01/004. arXiv:1910.01649

13. K. Saikawa, S. Shirai, Precise WIMP dark matter abundance and standard model thermodynamics. arXiv:2005.03544

14. E. Valenti, M. Zoccali, A. Mucciarelli, O.A. Gonzalez, F. Surot, D. Minniti et al., The central velocity dispersion of the milky way bulge. Astron. Astrophys. **616**, A83 (2018). https://doi.org/10.1051/0004-6361/201832905. arXiv:1805.00275

15. Y. Ascasibar, P. Jean, C. Boehm, J. Knoedlseder, Constraints on dark matter and the shape of the Milky Way dark halo from the 511-keV line. Mon. Not. R. Astron. Soc **368**, 1695 (2006). https://doi.org/10.1111/j.1365-2966.2006.10226.x. arXiv:astro-ph/0507142

16. Y. Rasera, R. Teyssier, P. Sizun, B. Cordier, J. Paul, M. Casse et al., Soft gamma-ray background and light dark matter annihilation. Phys. Rev. D **73**, 103518 (2006). https://doi.org/10.1103/PhysRevD.73.103518. arXiv:astro-ph/0507707

17. T .R. Slatyer, Indirect dark matter signatures in the cosmic dark ages. I. Generalizing the bound on s-wave dark matter annihilation from Planck results. Phys. Rev. D **93**, 023527 (2016). https://doi.org/10.1103/PhysRevD.93.023527. arXiv:1506.03811

18. M. Boudaud, T. Lacroix, M. Stref, J. Lavalle, Robust cosmic-ray constraints on p-wave annihilating MeV dark matter. Phys. Rev. D **99**, 061302 (2019). https://doi.org/10.1103/PhysRevD.99.061302. arXiv:1810.01680

19. Y. Ema, F. Sala, R. Sato, Light dark matter at neutrino experiments. Phys. Rev. Lett **122**, 181802 (2019). https://doi.org/10.1103/PhysRevLett.122.181802. arXiv:1811.00520

20. C. Cappiello, J .F. Beacom, Strong new limits on light dark matter from neutrino experiments. Phys. Rev. D **100**, 103011 (2019). https://doi.org/10.1103/PhysRevD.100.103011. arXiv:1906.11283

21. D. Banerjee et al., Dark matter search in missing energy events with NA64. Phys. Rev. Lett **123**, 121801 (2019). https://doi.org/10.1103/PhysRevLett.123.121801. arXiv:1906.00176

22. LDMX collaboration, Light Dark Matter eXperiment (LDMX). arXiv:1808.05219

23. K. Abazajian et al., CMB-S4 Science Case, Reference Design, and Project Plan. arXiv:1907.04473

24. Simons Observatory collaboration, The Simons Observatory: science goals and forecasts. JCAP **02**, 056 (2019). https://doi.org/10.1088/1475-7516/2019/02/056. arXiv:1808.07445

25. G. Krnjaic, Probing light thermal dark-matter with a Higgs portal mediator. Phys. Rev. D **94**, 073009 (2016). https://doi.org/10.1103/PhysRevD.94.073009. arXiv:1512.04119

26. P.B. Dev, R.N. Mohapatra, Y. Zhang, Revisiting supernova constraints on a light CP-even scalar. arXiv:2005.00490

27. E.W. Kolb, M.S. Turner, The early universe. Front. Phys. **69**, 1 (1990)

28. M. Baryakhtar, A. Berlin, H. Liu, N. Weiner, Electromagnetic signals of inelastic dark matter scattering. arXiv:2006.13918

29. K. Harigaya, Y. Nakai, M. Suzuki, Inelastic dark matter electron scattering and the XENON1T excess. arXiv:2006.11938

30. H.M. Lee, Exothermic dark matter for XENON1T excess. arXiv:2006.13183

31. J. Bramante, N. Song, Electric but not eclectic: thermal relic dark matter for the XENON1T excess. arXiv:2006.14089

32. I.M. Bloch, A. Caputo, R. Essig, D. Redigolo, M. Sholapurkar, T. Volansky, Exploring new physics with O(keV) electron recoils in direct detection experiments. arXiv:2006.14521

33. H. An, D. Yang, Direct detection of freeze-in inelastic dark matter. arXiv:2006.15672

34. S. Baek, J. Kim, P. Ko, XENON1T excess in local Z_2 DM models with light dark sector. arXiv:2006.16876

35. H.-J. He, Y.-C. Wang, J. Zheng, EFT analysis of inelastic dark matter for xenon electron recoil detection. arXiv:2007.04963

36. H. An, M. Pospelov, J. Pradler, A. Ritz, Directly detecting MeV-scale dark matter via solar reflection. Phys. Rev. Lett **120**, 141801 (2018). https://doi.org/10.1103/PhysRevLett.120.141801. arXiv:1708.03642

37. J.N. Bahcall, A.M. Serenelli, S. Basu, New solar opacities, abundances, helioseismology, and neutrino fluxes. Astrophys. J. Lett **621**, L85 (2005). https://doi.org/10.1086/428929. arXiv:astro-ph/0412440

38. R. Essig, M. Fernandez-Serra, J. Mardon, A. Soto, T. Volansky, T.-T. Yu, Direct detection of sub-GeV dark matter with semiconductor targets. JHEP **05**, 046 (2016). https://doi.org/10.1007/JHEP05(2016)046. arXiv:1509.01598

39. R. Essig, J. Mardon, T. Volansky, Direct detection of sub-GeV dark matter. Phys. Rev. D **85**, 076007 (2012). https://doi.org/10.1103/PhysRevD.85.076007. arXiv:1108.5383

40. B. Roberts, V. Dzuba, V. Flambaum, M. Pospelov, Y. Stadnik, Dark matter scattering on electrons: accurate calculations of atomic excitations and implications for the DAMA signal. Phys. Rev. D **93**, 115037 (2016). https://doi.org/10.1103/PhysRevD.93.115037. arXiv:1604.04559

41. B. Roberts, V. Flambaum, Electron-interacting dark matter: implications from DAMA/LIBRA-phase2 and prospects for liquid xenon detectors and NaI detectors. Phys. Rev. D **100**, 063017 (2019). https://doi.org/10.1103/PhysRevD.100.063017. arXiv:1904.07127

42. PANDAX collaboration, Limits on axion couplings from the first 80 days of data of the PandaX-II experiment. Phys. Rev. Lett. **119**, 181806 (2017). https://doi.org/10.1103/PhysRevLett.119.181806. arXiv:1707.07921